Photoluminescence fatigue and related degradation in thin-film photovoltaics

Diana Shvydka, C. Verzella, V. G. Karpov, and A. D. Compaan
*Department of Physics and Astronomy, University of Toledo, Toledo, Ohio 43606**

We observe that junction photoluminescence intensity (PL) excited by a constant power laser beam in polycrystalline CdTe/CdS solar cells gradually decreases similar to the PL fatigue in chalcogenide glasses. As a function of time it was studied at different laser beam powers and temperatures for contact-free and metallized regions. We were able to discriminate between the fatigue per se and concomitant short-time PL intensity drop due to the laser heating. The fatigue shows substantial variations between different spots on the sample. It is more profound at higher temperatures and laser beam powers where its value can be as large as 80 percent in two hours. At low temperatures and beam powers it saturates rather quickly not exceeding 10 percent of the initial PL intensity. We attribute the observed phenomenon to defect creation by the light-generated electrons and holes. The defects provide additional non-radiative recombination channels thus decreasing PL. Simultaneously, this negative feedback makes the defect-generation rate slowing down, so that the PL fatigue saturates. We propose a simple analytical model that fits the data.

PACS numbers: 73.00.00, 73.40.-c, 73.61.Ga, 78.20.-e, 78.55.Et, 78.55.-m

I. INTRODUCTION

Photoluminescence (PL) technique, often used to judge the material quality, is typically assumed to be a non-destructive method. This assumption does not always hold. In this work we find that in a polycrystalline CdTe/CdS solar cell, illuminated with a laser beam of constant power, junction photoluminescence intensity gradually decreases over time. This phenomenon is similar to the PL fatigue observed in chalcogenide glasses[1,2] and a number of other systems, such as GaAs[3–6], GaN[7], amorphous and porous Si[1,8,9], and quantum wells[10].

In the latter work, the observed fatigue amplitude was in some cases rather significant, up to 90% of the initial PL intensity during $\sim 100 \div 1000$ seconds, depending on the material, laser beam intensity, and temperature. No comparison between materials has been attempted and in each publication the PL fatigue was interpreted as though it was unique to a given system. Exponentials[2,6], stretched exponentials[8,9], and powers[4] were used to fit the fatigue temporal dependencies. One general believe in the above-cited work is that PL fatigue is due to defect accumulation. More specific hypotheses vary between different authors.

However, we note that overall, the fatigue kinetics data for different materials look similar. Hence, the same physical mechanism can be suspected behind the phenomenon in a variety of materials. Proposing such a mechanism is one of the goals here.

Our paper is organized as follows. In Section II we describe the experimental setup and data on PL fatigue. Section III introduces our model and comparison with the experiment. In Section IV we describe the fitting procedure and verify the model predictions. Extension of the model to other degradation processes is discussed in Section V. Section VI contains concluding remarks.

II. EXPERIMENTAL

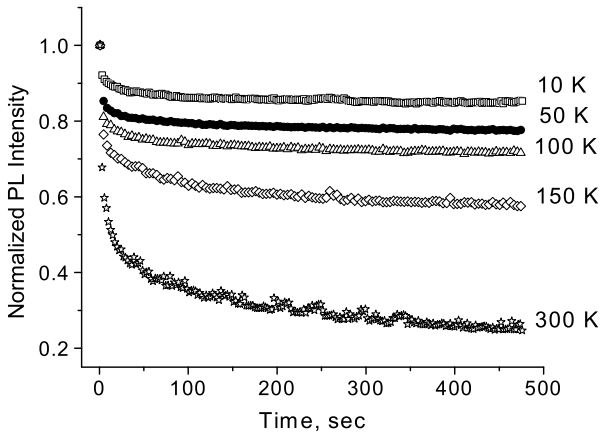

FIG. 1: Raw data on PL fatigue including laser heat contribution. Measured under the contact, laser power 25 mW ($\sim$ 1000 sun).

We conducted our experiment on CdTe/CdS solar cell made by vapor transport deposition as described in Refs. 11,17. These cells are thin-film junctions sandwiched between two electrodes, of which one is the transparent conductive oxide (TCO, ρ=15 $\Omega/\Box$) and the other is a metal of negligibly small resistance. Some of this structures remained unfinished, without a metal contact on top of CdTe layer. This provision made it possible to study the back contact effect on PL decay (it was shown indeed[12] that the presence of surface metal can effect the PL signal).

PL was excited from the glass side with 752 nm line of Kr laser. In this case, CdS is transparent to the laser light, which is absorbed in CdTe with an absorption length of ~ 0.3 μm. This is much narrower than the depletion layer width $\sim 1 \div 3$ μm in the lightly p-doped

CdTe. Hence, both the absorption and emission are restricted to a narrow junction region. The laser beam diameter was less than 0.1 mm. PL intensity change with time was recorded with CCD camera for several different temperatures and laser intensities.

We start with separating out the PL fatigue from the concomitant heat induced PL decrease. Shown in Fig 1 is an example of 'raw' data corresponding to different temperatures. Each of the curves shows relatively fast initial drop followed by more gradual decay. The initial drop rather independent on the sample temperature was attributed to the laser heating effect on the temperature dependent PL intensity in CdTe film as explained below. We find it important to subtract the laser heating effect, which otherwise masks the PL fatigue trends and makes it hard to interpret.

The reasoning behind the laser heat subtraction is that (i) the PL intensity in CdTe has a considerable temperature dependence (as verified in Fig. 2) and (ii) the characteristic time of establishing the stationary temperature distribution ($\sim$ 1 s, see the Appendix) is comparable to that of the observed initial PL intensity drop in Fig 1.

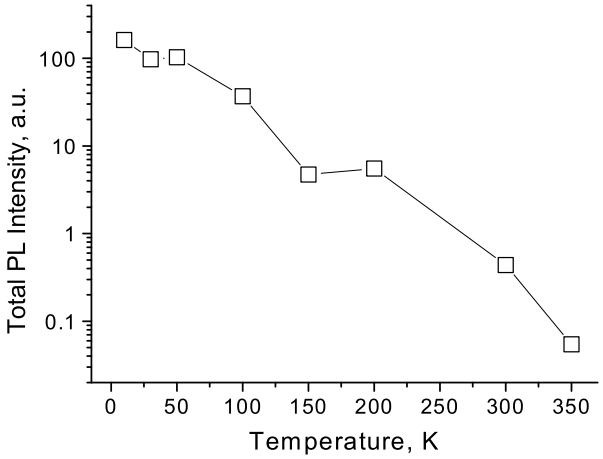

FIG. 2: Temperature dependence of total PL intensity in CdS/CdTe device.

To additionally verify the laser heat effect on PL intensity we implemented a setup where the sample was placed on a moving stage. In this setup the laser beam spot moved relative to the stage by a distance of its diameter in a time of the order of 0.5 s, shorter than the characteristic temperature equilibration time. At room temperature we observed the PL intensity drop by the factor of 1.5 in a matter of seconds after the stage seized to move. This is consistent with the laser heating effect: the beam fixed on a particular spot increases the spot temperature, thus decreasing PL, in accordance with the data in Fig. 2.

Using the same setup we were able to verify the nonlocal character of PL fatigue in the course of cyclical laser beam scanning as follows. First, we measured PL intensity along two parallel lines 3 mm apart on the sample.

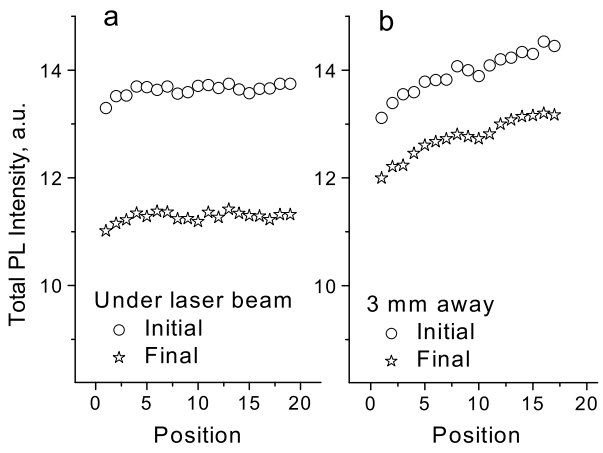

FIG. 3: Degradation of PL signal in laser cycling experiment a) directly under laser beam vs b) 3 mm away from the laser beam. Horizontal axes show the laser beam position along the scan line.

Then we performed periodical laser scanning along one of these lines. After 12 cycles we detected PL fatigue not only along the scanned line, but also along the unstressed second line (Fig. 3). The latter nonlocal PL fatigue effect can be understood assuming that the decrease is due to material degradation caused by the laser-generated nonequilibrium charge carriers, which as shown in Ref. 13 propagate far from the laser beam in the lateral direction. The fact that the nonlocal effect was weaker we attribute to the laser-induced heating with relatively short localization radius (see the Appendix): higher temperature directly under the beam lead to the fatigue acceleration along the laser trajectory line.

Shown in Fig. 4 is a set of typical PL fatigue data corrected to the laser heating effect and normalized to the initial PL intensity. Our heating subtraction procedure was based on the observed drastic change in logarithmic derivatives of the PL decay temporal dependencies. We identified that change with the characteristic temperature equilibration time and eliminated the data corresponding to shorter times.

We observed the following trends: (1) the fatigue accelerates and its amplitude increases with temperature and laser beam power; (2) there are considerable variations in the PL fatigue amplitude (up to 100%) between different spots on the sample, especially for metal-free area (consistent with the observed fluctuations in solar cell efficiency degradation[14]); (3) there is no significant difference in the fatigue kinetics between metal-free and metallized regions; (4) the fatigue spreads beyond the laser spot region affecting areas up to several mm away from the spot; (5) PL fatigue kinetics are not very different in the open circuit and shorted samples, in spite of the fact that the former shows considerably higher PL intensity.[15]

Some of the above items, such as beam power depen-

dence and nonlocal degradation, are similar to the observations for other materials. Other facts, such as variations between different spots and independence of back contact are observed here for the first time.

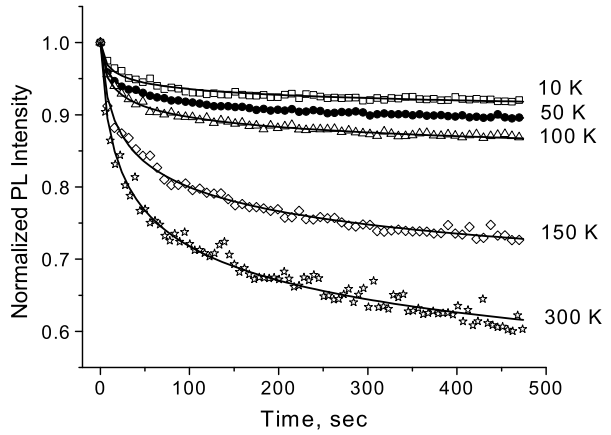

FIG. 4: Data on PL fatigue without the laser heating effect. Contact area, laser power 25 mW. Solid lines represent fits by Eq. (11) and Eq. (12.

)

III. MODEL

We attribute the observed PL fatigue to defects generated under illumination. While photons do not have enough energy to create the defects, the light-generated electrons and holes are capable of defect generation, which is considered a mechanism underlying photo-induced degradation in many cases[16]. In particular, it was experimentally verified for the case of CdTe photovoltaics that light-generated electrons and holes, rather than the light per se, are responsible for degradation.[17]

In the simplest approximation the defect generation rate is linear in the charge carrier concentration n (a defect is generated by capturing single electron or hole on some cite) that is

$$\frac{dN}{dt} = \alpha n - \beta N. \tag{1}$$

Here α and β are material parameters, the two terms in the right-hand side describe defect creation and annihilation. In turns, the electron kinetics depends on defect concentration (N) and built-in junction electric field $\mathcal{E}$,[15]

$$G(x) = \gamma n N + \mu \mathcal{E} \frac{\partial n}{\partial x}. \tag{2}$$

Here

$$G(x) = G_0 \Theta(x) \exp(-x/l)$$

is the electron-hole generation rate ($\mathrm{cm^{-3}s^{-1}}$), l is the absorption length, μ is the mobility, $\Theta(x)$ is the step function ($x > 0$ corresponds to CdTe), γ is a constant. In the right-hand side of Eq. (2) the first term accounts for the electron recombination via defects, while the second one describes the charge carrier drift caused by the junction electric field. In Eq. (2) we have taken into account that the electron kinetics is fast (as compared to that of the defects) and thus can be described in the quasistationary approximation.

Eqs. (1) and (2) reduce to a complex mathematical problem that in the generation region $x \leq l$ can be simplified by employing the approximations[18]

$$G(x) = const \equiv G, \quad \frac{1}{n}\frac{\partial n}{\partial x} = l^{-1}. \tag{3}$$

As a result Eq. (2) takes an intuitively clear form

$$n = G\tau, \quad \frac{1}{\tau} = \frac{1}{\tau_N} + l^{-1}\mu\mathcal{E}, \tag{4}$$

where the two last terms describe the probabilities per unit time for the carrier to recombine non-radiatively ($1/\tau_N \equiv \gamma N$) or to be swept out by the field from the generation region.

Eqs. (1) and (4) have a closed solution which is still arithmetically cumbersome. To make it more intuitive we start with considering the fatigue early stage. Neglecting the annihilation term in Eq. (1) gives

$$n(t) = n_0 \left(1 + \frac{t}{\theta}\right)^{-1/2} \tag{5}$$

where

$$n_0 = \frac{G\tau_0}{1 + l^{-1}\mu\tau_0\mathcal{E}}, \quad \theta = \frac{G}{2\alpha\gamma n_0^2}. \tag{6}$$

Here $\tau_0 \equiv 1/\gamma N_0$ and N_0 is the initial defect concentration.

Furthermore, the initial stage of fatigue can be similarly described for a higher order kinetics, $dN/dt = \alpha n^\eta$ to give

$$n(t) = n_0 \left(1 + \frac{t}{\theta}\right)^{-1/(\eta+1)}, \quad \theta = \frac{G}{\alpha\gamma(\eta+1)n_0^{\eta+1}}. \tag{7}$$

We observe that functionally the temporal kinetics is field-independent. However, its characteristic time, θ depends on the field via the initial carrier concentration, in accordance with Eq. (6).

Note that the temporal dependence in Eq. (7) was successfully used to fit the PL fatigue in GaAs.[4] From more general prospective, it is important that the built-in electric field does not affect the shape of the initial PL fatigue temporal kinetics. In particular, this makes our consideration applicable to some crystals where short absorbtion length restricts PL to a near surface region of significant electric field.[3,6] As long as the electric field does not affect the kinetics, the data corresponding to different systems (bulk PL, near-surface PL, junction PL) can be all analyzed within the same framework.

The fatigue late stage can be described by setting the time derivative zero in Eq. (1), which gives the saturated charge carrier concentration n_s,

$$n_s = \frac{G}{\gamma N_\infty}\left\{\left[\left(\frac{\mu\mathcal{E}}{2\gamma l N_\infty}\right)^2+1\right]^{1/2}-\frac{\mu\mathcal{E}}{2\gamma l N_\infty}\right\} \quad (8)$$

Here

$$N_\infty = \left(\frac{\alpha G}{\gamma\beta}\right)^{1/2}. \quad (9)$$

is the ultimate defect concentration accumulated after infinitely long time in the absence of field. Note that in a strong field, $\mathcal{E} \gg \gamma l N_\infty/\mu$ the carrier concentration does not degrade, $n_s = n_0 = Gl/\mu\mathcal{E}$. In a rough approximation, the charge carrier evolution can be described by combining Eqs. (5) and (9),

$$n(t) = (n_0 - n_s)\left(1+\frac{t}{\theta}\right)^{-1/2} + n_s. \quad (10)$$

We attribute the observed PL fatigue to the time decay in the charge carrier concentration and assume the radiative recombination kinetics bilinear in the electron and hole concentrations, $I \propto n_e n_h$. In particular, using Eq. (6) to describe n_e and n_h gives an accurate result for the bias-dependent PL intensity[15].

While I is bilinear in $n_e n_h$, the two type carrier kinetics can be significantly different owing to the difference in their parameters. For example, the hole drift mobility in CdTe is by order of magnitude lower than that of electrons. In addition, holes typically stronger interact with the atomic system thus being more capable of creating the defects. Therefore, the details of the fatigue kinetics can be different in different systems depending on the charge carrier parameters.

From this point on we narrow the model to reflect the specificity of our data. The key observation is that the fatigue kinetics is almost the same under open- and short-circuit cases. Hence, the junction electric field, different for the above two cases, does not affect the defect generation and underlying charge carrier kinetics (we recall that PL is emitted from the junction region).

On the other hand, the bias dependent PL exhibits a seemingly conflicting observation of the charge carrier kinetics sensitive to the junction electric field.[15] To reconcile the two facts we attribute them to two different types of carriers, electrons and holes, which reaction to the field and defect generation abilities can be significantly different. It is likely that mobile electrons are effectively swept away by the field, while the holes spend more time in the junction region and generate defects causing the PL fatigue.

Consider the extreme case where the carriers of one type (n_h) are immobile and fully responsible for defect generation, while the alternative mobile carriers (n_e) are swept away from the junction region. In this case the PL intensity can be represented as

$$I(t) \propto n_h(t) n_e(0) \propto \frac{n_h(t)}{1 + l^{-1}\mu_e\tau_{0e}\mathcal{E}}, \quad (11)$$

where $n_h(t)$ is given by Eq. (5) or Eq. (12) below. This form enables one to simultaneously describe the bias-dependent PL intensity and PL fatigue.

Assuming the fatigue kinetic field independent, Eqs. (1) and (4) can be solved for n to give[11]

$$n = \frac{G}{\gamma N_\infty}\left\{1-\left[1-\left(\frac{N_0}{N_\infty}\right)^2\right]\exp\left(-2\beta t\right)\right\}^{-1/2}. \quad (12)$$

When the time is relatively short, $\beta t \ll 1$ the latter result takes the form of Eq. (5) with

$$\theta \equiv \frac{1}{2\beta}\frac{N_0^2}{N_\infty^2 - N_0^2}. \quad (13)$$

Note that θ is generally temperature dependent as it includes the coefficients α (through N_∞), and β which describe the probability of electron-triggered atomic rearrangements. The typical dependence of that kind is thermally activated above the Debye temperature and is weaker at lower temperatures.[19]

IV. FITTING THE DATA

Assuming, on empirical grounds, a significant asymmetry between the electrons and holes we used Eq. (11) with Eq. (12) for $n_h(t)$ to fit the data. As shown in Fig. 4, good agreement is achieved.

We have verified several predictions of the above model addressing the main curve parameters, the fatigue initial slope ($d\ln I/dt = 1/2\theta$) and relative saturated value ($I(\infty)/I(0)$) versus temperature and generation rate G proportional to the laser power in our experiment. The predictions are:

$$\frac{1}{2\theta} = \beta\left[\left(\frac{N(\infty)}{N(0)}\right)^2 - 1\right] = \beta\left(\frac{\alpha G}{\gamma\beta N_0^2} - 1\right), \quad (14)$$

$$\frac{I(\infty)}{I(0)} = \frac{N(0)}{N(\infty)} = \left(\frac{\gamma\beta N_0^2}{\alpha G}\right)^{1/2}. \quad (15)$$

The data in Figs. 5, 6 are qualitatively consistent with Eqs. (14), (15), which predict increase in the initial slope and decrease in the relative saturated value with T and G. We note that the above relations combine into

$$\frac{1}{2\theta}\left[1-\left(\frac{I(\infty)}{I(0)}\right)^2\right]^{-1} = \beta \quad (16)$$

where the right-hand-side can depend on T, but not on G. The latter prediction is verified in Fig. 7, where temperature dependence is obscured by spot-to-spot PL fatigue variations (note, that each point in Fig. 7 is taken at a different spot on the sample).

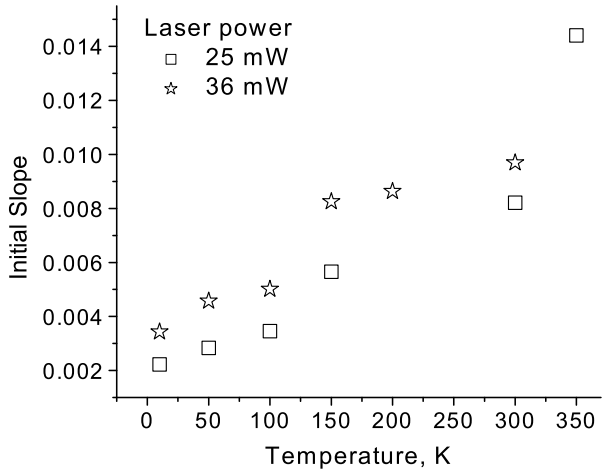

FIG. 5: Dependence of the initial PL fatigue slope on temperature for different laser beam powers.

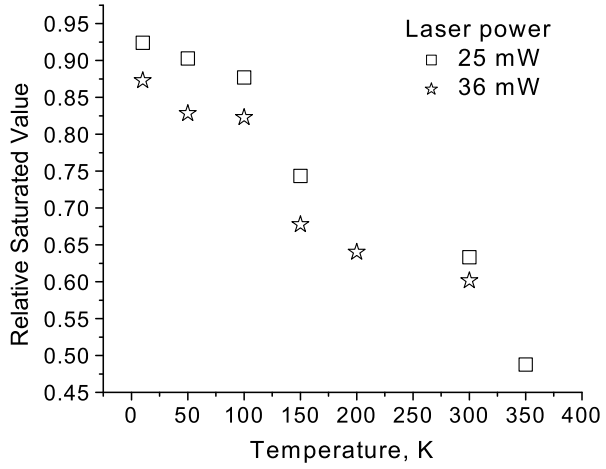

FIG. 6: Temperature dependence of the relative saturated value for different laser beam powers.

V. RELATED DEGRADATION PHENOMENA

Closely related to the PL fatigue is the phenomenon of light-induced degradation known to be a significant problem for thin-film photovoltaics. A minor difference is that sun light has a broad spectrum and thus generates the nonequilibrium charge carriers more uniformly in space. In the uniform generation approximation, l in the above equations represents the junction thickness rather than the absorption length. Also, for the case of practically important relatively small degradation, the photovoltaic characteristics change approximately linear with the charge carrier concentration. With these modifications, and generalizing Eq. (7) the relative degradation of the major photovoltaic parameters X, such as short circuit current ($X = J_{sc}$), open circuit voltage ($X = V_{oc}$), and efficiency ($X = E$) will all have the same temporal

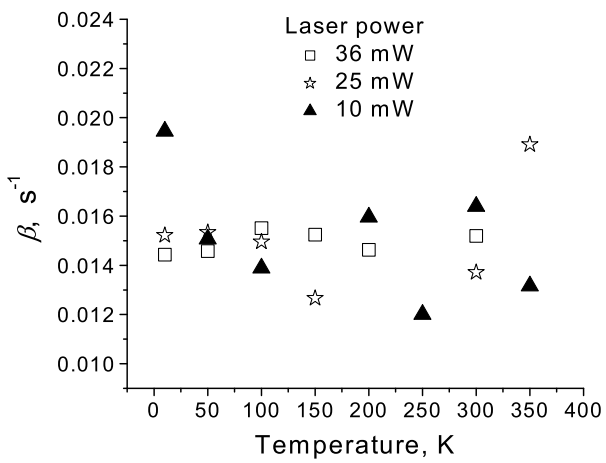

FIG. 7: Probability of defect annihilation β vs. temperature: independent of laser power.

dependence

$$\frac{\Delta X}{X} \propto \left(1+\frac{t}{\theta}\right)^{-\eta/(\eta+1)}, \quad \theta \propto \frac{(1+\mathcal{E}/\mathcal{E}_c)^{\eta+1}}{\alpha\gamma G^{\eta}}. \quad (17)$$

Here the characteristic field $\mathcal{E}_c \equiv l/\mu\tau_0$ is related to the recombination time, which is known to depend on the carrier generation rate[20]. In particular, $\mathcal{E}_c$ can be much lower (and τ_0 much longer) far from metallurgical junction. Correspondingly, the sun light induced degradation can be more sensitive to the electric field than PL fatigue.

Eq. (17) contains a number of verifiable predictions. (i) Specific temporal dependence with a tendency to saturation. (ii) Temperature dependence of the time scale θ related to the product $(\alpha\gamma)^{-1}$ exponential in T at temperatures higher or of the order of the Debye temperature (Note that the latter dependence is not predicted for the absolute value of degradation, whose temperature dependence is often addressed.[21]) (iii) Field dependence, which predicts the short circuit device (maximum $\mathcal{E}$) to degrade less than the open circuit one ($\mathcal{E}$ is suppressed), consistent with observations.[22,23]

From the practical standpoint, it is important that a variety of charge carrier driven degradation phenomena possess the same temporal, field, and temperature dependencies. This opens a venue for predictive modelling and accelerated life testing where one source of degradation is replaced by another, for example, relatively fast laser or electron beam induced degradation instead of long term one-sun-light degradation. As an illustration, in Fig. 8 we compare properly rescaled degradation kinetics caused by all three of the latter sources: good qualitative agreement is observed.[24]

A comment is in order regarding charge carrier triggered degradation in laterally nonuniform systems.[17] The nonuniformity screening by charge carriers depends on their concentration,[13] which is different for different sources. This will eventually result in the correspondingly different degradations. Indeed, the nonuniformity

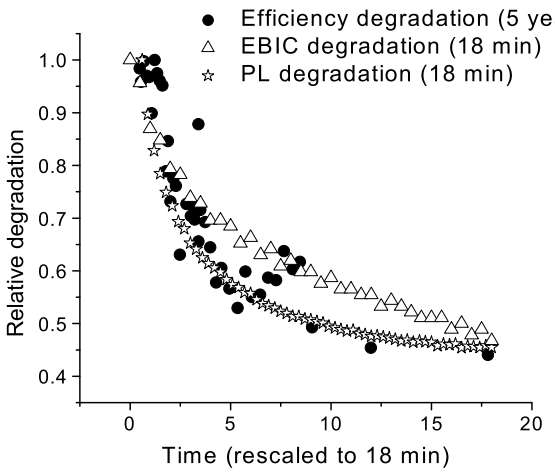

FIG. 8: Comparison of the light-induced (1 sun) efficiency degradation, e-beam-induced (15 keV) EBIC degradation and laser-beam-induced (1000 sun) PL degradation. Data rescaled to 18 min.[24]

showed up in our experiments as considerable fluctuations in the fatigue effect between different spots. The above idea of accelerated life testing cannot be deterministically predictive for nonuniform systems, such as amorphous, porous, and polycrystalline materials. However, for such systems the accelerated testing results interpreted statistically may characterize the trends in degradation phenomena.

VI. CONCLUSIONS

In conclusion, the decay in the PL excited by a stationary laser beam in CdTe photovoltaics is for the first time observed. Two decay sources are identified: short-term laser induced heating decreasing PL intensity, and long-term material degradation (fatigue) due to photoinduced defect accumulation. The fatigue exhibits such trends as acceleration with the temperature and light intensity, considerable variations between different spots on the sample, and nonlocal nature of the effect. Similarities with the PL fatigue in a number of other systems are found.

Our theoretical model applies to a variety of materials and attributes the PL fatigue to defects generated by the nonequilibrium electrons and holes. The model gives correct predictions about the fatigue temperature, light intensity, and field dependencies.

Our understanding predicts the same physics underlying nominally different degradation phenomena, such as caused by the laser beam, electron beam, and sun light. This opens a venue for accelerated life testing where long term sun-light induced degradation is simulated by short term degradations caused by laser or electron beams, or electric bias. The similarity can be obscured by material nonuniformity effects. More study is called upon to clarify this practically important issue.

Acknowledgments

This work was partially supported by NREL, Grant No NDJ-1-30630-02. One of us (C. V.) acknowledges the support from NSF-REU, Grant PHY-0097367.

APPENDIX

In this appendix we consider the temperature distribution caused by the laser beam, which we model as a cylindrical heat source across the film of small thickness h attached to a relatively thick metal slab ('cold finger') of thickness H. The thermal conductivities of the two materials are κ and K respectively (Fig. 9). The temperature T_0 is maintained at the opposite side of the system. We assume the heat source of small radius as compared to the below derived thermal nonuniformity decay length λ. The heat transfer is then described by the equation

$$h\kappa \frac{1}{r}\frac{\partial}{\partial r} r \frac{\partial T}{\partial r} = -K\frac{T-T_0}{H}, \tag{A.1}$$

where r is the distance from the cylinder axis. This gives the temperature decay length

$$\lambda = \sqrt{\frac{\kappa}{K} Hh} \tag{A.2}$$

For numerical estimates at room temperature we take $k \approx 0.1$ W/cm-^{o}C, $h \sim 3$ μm and consider copper slab of $H = 1$ cm and $K \approx 4$ W/cm-^{o}C. This gives $\lambda \sim 0.03$ mm, larger than our laser beam radius.

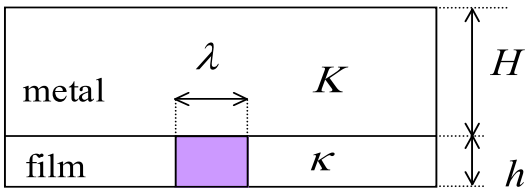

FIG. 9: Parameters describing heat transfer from a cylindrical source in thin film in contact with a metal slab.

To estimate the temperature nonuniformity amplitude δT caused by a source of power P consider the heat transfer equation

$$P = 2\pi\lambda h\kappa \frac{\partial T}{\partial r} \approx 2\pi h\kappa \delta T. \tag{A.3}$$

For typical $P \sim 10$ mW this gives $\delta T \sim 50$ K.

Finally, to estimate the thermal conduction equilibration time

$$\tau \sim \frac{H^2 C\rho}{K} \tag{A.4}$$

we use the copper specific heat $C \approx 400$ J/kg-K and the density $\rho \approx 10$ g/cm^3, which give $\tau \sim 1$ s.

---

* Electronic address: dshvydka@physics.utoledo.edu

[1] R.A. Street, Phys. Rev. B **17**, p.3984 (1978).

[2] T. N. Mamontova and A. V. Chernyshev, Soviet Physics - Semiconductors **18**, 332 (1984).

[3] D. Guidotti, Eram Hasan, H.J. Hovel, and Marc Albert, Appl. Phys. Lett. **50**, 912 (1987).

[4] M.Y.A. Raja, S.R.J. Brueck, M. Osinski, and J. McInerney, Appl. Phys. Lett. **52**, 625 (1988).

[5] D. Guidotti and H.J. Hovel, Appl. Phys. Lett. **53**, 927 (1988).

[6] D. Guidotti and H.J. Hovel, Appl. Phys. Lett. **53**, 1411 (1988).

[7] Bosang Kim, I. Kuskovsky, Irving P. Herman, D.Li, and G.F. Neumark, J. Appl. Phys. **86**, 2034 (1999).

[8] R. Laiho, A. Pavlov, and O. Hovi, T. Tsuboi, Appl. Phys. Lett. **63**, 275 (1993).

[9] I. M. Chang, S. C. Pan, and Y. F. Chen, Phys. Rev. B **48**, 8747 (1993).

[10] G.M Haugen, S. Guha, H. Cheng, J.M. DePuydt, M.A. Haase, G.E. Hofler, J. Qiu, and B.J. Wu, Appl. Phys. Lett. **66**, 358 (1995).

[11] R.Harju, V.G. Karpov, D. Grecu, and G. Dorer, J. Appl. Phys. **88**, 1794 (2000).

[12] D. H. Levi, L. M. Woods, D. S. Albin, T. A. Gessert, R. C. Reedy, and R. K. Ahrenkiel, in *Proceedings 2d World Conference on Photovoltaic Solar Energy Conversion*, Vienna, Austria (1998), available at www.nrel.gov/ncpv/pdfs/levi.pdf.

[13] Diana Shvydka, A. D. Compaan and V. G. Karpov, J. Appl. Phys. **91**, 9059 (2002).

[14] Bolko von Roedern, Mat. Res. Soc. Symp. Proc. **668**, p.H6.9.1 (2001).

[15] Diana Shvydka, V. G. Karpov, and A. D. Compaan, Appl. Phys. Lett. **80**, 3114 (2002).

[16] D. Redfield and R. Bube, *Photoinduced Defects in Semiconductors*, Cambridge, University Press 1996.

[17] V. G. Karpov, A. D. Compaan, and Diana Shvydka, Appl. Phys. Lett. **80**, 4256 (2002).

[18] The derivative estimate is valid since the length $\alpha^{-1} \approx 0.3$ μm is much shorter than the characteristic drift and diffusion lengths ($\sim 1 \div 3$ μm) in the material.

[19] H. Sher and T. Holstein, Phil. Mag., **B**, **44**, 343 (1981).

[20] S.M. Sze *Physics of Semiconductor devices*, John Wiley and Sons, New York, 1981.

[21] J.F. Hiltner and J.R. Sites, *AIP Conf. Proc.* **462**, 170 (1998).

[22] S. S. Hegedus, B. E. McCandles, and R. W. Birkmire, *Proceedings 28th IEEE Photovoltaic Specialists Conference*, Alaska, 2000, p. 535.

[23] Our consideration does not describe degradation under significant reverse bias, which mechanism can be different (for example, electromigration or localized charge carrier generation through the Frantz - Keldysh effect).

[24] Linear rescaling was performed in such a way, that initial and final data points were superposed for all three degradation curves. In particular, the final relative degradation in Fig. 8 does not show the actual efficiency and EBIC (electron beam induced current) degradation absolute values.